Author Manuscript Published OnlineFirst on August 4, 2016; DOI: 10.1158/1078-0432.CCR-16-0520
Author manuscripts have been peer reviewed and accepted for publication but have not yet been edited.

Loss of SMAD4 Promotes Lung Metastasis of Colorectal Cancer by Accumulation of CCR1$^+$ Tumor-associated Neutrophils through CCL15-CCR1 Axis

Takamasa Yamamoto[1], Kenji Kawada[1]*, Yoshiro Itatani[1,2,5], Susumu Inamoto[1], Ryosuke Okamura[1], Masayoshi Iwamoto[1], Ei Miyamoto[3], Toyofumi F Chen-Yoshikawa[3], Hideyo Hirai[4], Suguru Hasegawa[1], Hiroshi Date[3], Makoto M. Taketo[1,2], Yoshiharu Sakai[1]

Authors' Affiliations: Departments of Surgery[1], Pharmacology[2], Thoracic surgery[3], and Transfusion Medicine & Cell Therapy[4], Graduate School of Medicine, Kyoto University, Kyoto 606-8507, Japan.

[5]Moores UCSD Cancer Center, University of California, San Diego, La Jolla, California 92093, U.S.A.

Corresponding author: Kenji Kawada, Department of Surgery, Graduate School of Medicine, Kyoto University, 54 Shogoin- Kawara-cho, Sakyo-ku, Kyoto, Japan, 606-8507.

Phone: +81-75-366-7595; FAX: +81-75-366-7642; E-mail: kkawada@kuhp.kyoto-u.ac.jp

Running title: Lung metastasis of colorectal cancer through CCL15-CCR1 axis

Key words; Colorectal cancer, lung metastasis, SMAD4, myeloid cells, tumor microenvironment,

Grant Support: This study was supported by grants from the Ministry of Education, Culture, Sports, Science and Technology of Japan (grant number 24591975), from Japan Research Foundation for Clinical Pharmacology, and from Mochida Memorial Foundation for Medical and Pharmaceutical Research (to K. Kawada).

The costs of publication of this article were defrayed in part by the payment of page charges. This article must therefore be hereby marked *advertisement* in accordance with 18 U.S.C. Section 1734 solely to indicate this fact.

Potential Conflict of Interest: No potential conflicts of interest were disclosed.

Word Counts: 4305 words

Figures and tables: 3 figures and 3 tables

Supplementary figures and tables: Supplementary 6 figures

Statement of translational relevance

Tumor microenvironment contains several types of cells including cancer cells and normal host cells. The use of various mouse models has shown that bone marrow-derived myeloid cells, such as tumor-associated macrophages (TAMs), myeloid-derived suppressor cells (MDSCs) and tumor-associated neutrophils (TANs), have important roles in tumor progression. However, it remains to be determined whether similar mechanisms are involved in humans. We have recently reported loss of SMAD4 stimulates expression of chemokine CCL15 from colorectal cancer (CRC) to recruit $CCR1^+$ MDSCs, which promotes tumor invasion of primary CRC. This is the first clinical study showing that loss of SMAD4 promotes lung metastasis of CRC by accumulation of $CCR1^+$ TANs through the CCL15-CCR1 axis, and that CCL15 expression of lung metastatic lesions is an independent predictor of worse prognosis in CRC patients. These results may justify the treatment with CCR1 inhibitors to prevent lung metastasis of CRC after pulmonary resection of metastatic CRC.

Abstract

Purpose: We have reported loss of SMAD4 promotes expression of CCL15 from colorectal cancer (CRC) to recruit $CCR1^+$ myeloid cells through the CCL15-CCR1 axis, which contributes to invasion and liver metastasis. However, the molecular mechanism of lung metastasis is yet to be elucidated. Our purpose is to determine whether similar mechanism is involved in the lung metastasis of CRC.

Experimental Design: In a mouse model, we examined whether SMAD4 could affect the metastatic activity of CRC cells to the lung through the CCL15-CCR1 axis. We immunohistochemically analyzed expression of SMAD4, CCL15 and CCR1 with 107 clinical specimens of CRC lung metastases. We also characterized the $CCR1^+$ myeloid cells using several cell-type specific markers.

Results: In a mouse model, CCL15 secreted from SMAD4-deficient CRC cells recruited $CCR1^+$ cells, promoting their metastatic activities to the lung. Immunohistochemical analysis of lung metastases from CRC patients revealed that CCL15 expression was

significantly correlated with loss of SMAD4, and that CCL15-positive metastases recruited ~1.9 times more numbers of $CCR1^+$ cells than CCL15-negative metastases. Importantly, patients with CCL15-positive metastases showed a significantly shorter relapse-free survival (RFS) than those with CCL15-negative metastases, and multivariate analysis indicated that CCL15 expression was an independent predictor of shorter RFS. Immunofluorescent staining showed that most $CCR1^+$ cells around lung metastases were tumor-associated neutrophil (TAN), although a minor fraction was granulocytic myeloid-derived suppressor cell (granulocytic-MDSC).

Conclusion: CCL15-CCR1 axis may be a therapeutic target to prevent CRC lung metastasis. CCL15 can be a biomarker indicating poor prognosis of CRC patients with lung metastases.

Introduction

Colorectal cancer (CRC), one of the most common cancers worldwide, frequently metastasizes to the liver and lung. The lung is one of the most frequent sites of metastases from CRC, with an incidence of approximately 5–15% (1, 2, 3). Although the development of chemotherapy for metastatic CRC has been reported, surgical resection of lung metastases appears the most optimal treatment, if possible (4). It was reported that complete pulmonary resection can improve the 5-year survival rate up to more than 45% (5-9). However, there are few unified criteria for surgical resection for lung metastases.

To achieve comprehensive therapeutic effects, it is imperative to understand the molecular mechanisms behind individual cancers. Studies in various mouse models have shown that bone marrow-derived myeloid cells, such as tumor-associated macrophages (TAMs), myeloid-derived suppressor cells (MDSCs) and tumor-associated neutrophils (TANs), play important roles in tumor progression (10-14). For example, Lyden and colleagues reported that hematopoietic progenitor cells expressing myeloid cell marker (CD11b) and vascular endothelial growth factor receptor 1 (VEGFR1)

accumulate at the premetastatic niche in the lung to form cellular clusters and promote tumor metastasis through the VEGF/VEGFR1 and CXCL12/CXCR4 pathways (10). Moses and colleagues reported that a mutant form of transforming growth factor-β (TGF-β) receptor recruits MDSCs ($CD11b^+$ $Gr\text{-}1^+$) at the tumor invasion front via CXCL12/CXCR4 and CXCL5/CXCR2 axes, contributing to lung metastasis of breast cancer (11). However, most of these findings were obtained from mouse models, and it remains to be determined whether such mechanisms are actually involved in humans.

SMAD4 is a key mediator of the TGF-β superfamily signaling, and acts as a tumor suppressor in CRC. Loss of SMAD4 protein expression is found in 20–40% of CRC cases, and strongly correlated with the prognosis of CRC patients (15-18). We previously showed that in *cis-Apc*$^{+/\Delta 716}$ *Smad4*$^{+/-}$ (*Apc/Smad4*) mice that develop invasive intestinal adenocarcinomas, mouse CCL9 (mCCL9) is secreted from the cancer epithelium, which recruits myeloid cells expressing its receptor CCR1 (19, 20). Using a mouse model of CRC liver metastasis, we also demonstrated that mCCL9-expressing CRC cell lines recruit $CCR1^+$ myeloid cells to expand metastatic foci in the liver (21), and that four distinct types of myeloid cells are recruited to the metastatic foci; $CCR1^+$ neutrophils,

eosinophils, monocytes and fibrocytes (22). In addition to these mouse models, we recently reported that SMAD4 binds directly to the promoter region of human *CCL15* gene (a human ortholog of mouse *CCL9*) and negatively regulates its expression (23). Using human clinical specimens, we also showed that loss of SMAD4 promotes CCL15 expression to recruit $CCR1^+$ myeloid cells and facilitates primary tumor invasion and liver metastasis of CRC (23, 24). Most $CCR1^+$ cells accumulating at the invasion front of primary CRC were of the MDSC phenotype ($CD11b^+$, $CD33^+$, and $HLA\text{-}DR^-$) (24). Importantly, patients with CCL15-expressing liver metastases showed significantly shorter relapse-free survival (RFS) than those with CCL15-negative ones ($P = 0.04$) (23). Stage II/III patients with CCL15-positive primary CRC tended to have shorter RFS than those with CCL15-negative CRC ($P = 0.15$), although not a significant difference (24). However, it has not been investigated whether the CCL15-CCR1 chemokine axis is involved in lung metastasis of CRC.

Here we report that in human clinical specimens, SMAD4-deficient lung metastases of CRC showed a significant correlation with CCL15 expression, which was associated with $CCR1^+$ cell accumulation. Most of the $CCR1^+$ cells accumulating around the lung

metastases were of the TAN phenotype ($CD11b^+$, $CD33^-$, $HLA\text{-}DR^-$, $CD15^+$ and $CD16^+$), although some were of the granulocytic-MDSC phenotype ($CD11b^+$, $CD33^+$, $HLA\text{-}DR^-$ and $CD15^+$). Importantly, CRC patients with CCL15-positive lung metastases exhibited a significantly shorter RFS than those with CCL15-negative ones (P = 0.022). We also found that CCL15 expression of lung metastases could be a significant predictor of shorter RFS, as determined by multivariate Cox proportional hazards model analysis. In a mouse model of lung metastasis, SMAD4-deficient CRC cells showed high capacity of metastasis to the lung, which was suppressed by the treatment of CCR1 inhibitor. These results suggest that blocking the CCL15-CCR1 axis may provide a novel therapeutic strategy for lung metastases of CRC, and that CCL15 expression may be a novel predictive biomarker of CRC patients with lung metastases.

Materials and Methods

Patients' population

A total of 107 lung metastases were obtained from 81 CRC patients undergoing pulmonary resection at Kyoto University Hospital between 2006 and 2013, and their tissue samples were retrospectively analyzed. The diagnosis of CRC was confirmed by pathological examination. The study protocol was approved by the institutional review board of Kyoto University, and the patients provided their consents for data analysis.

Cell lines and reagents

HT29 and HCT116 cells were supplied from American Type Culture Collection (ATCC) in the year 2011 during study initiation and were maintained in low glucose DMEM with 10% fetal bovine serum and 1% penicillin/streptomycin mixture. All cell lines were authenticated by TAKARA Bio Inc (Shiga, Japan) using DNA profiling of short tandem repeat markers and further verified by morphology and/or flow cytometry on July, 2014. They were routinely tested negative for *mycoplasma*. Stable transductants of HT29 cells for firefly luciferase and cMyc-tagged human *SMAD4* were established, as

previously described (23, 24). Stable transductants of HCT116 cells for firefly luciferase and shRNA against *SMAD4* (sh*SMAD4*) were established, as previously described (23). A detailed list of the antibodies used was reported previously (23, 24). Anti-CD16 mouse antibody was obtained from Leica Biosystems (Wetzlar, Germany) and anti-Luciferase goat antibody from Promega (Fitchburg, WI).

Quantitative reverse transcription polymerase chain reaction (qRT-PCR)

Total RNA was extracted using RNeasy Mini kit (Qiagen, Hilden, Germany) according to the manufacturer's protocol. Complementary DNA generated by reverse transcription was quantified using ABI PRISM 7700 (Applied Biosystems, Carlsbad, CA). The primer-probe sets for *CCL15* and *ACTB* were from TaqMan Gene Expression assays (assay ID, Hs00361122_m1 and Hs99999903_m1, respectively). The mRNA level for *CCL15* was normalized to that for *ACTB* by a ΔCt method.

Western blotting

Cells were lysed in NP-40 lysis buffer (20 mM Tris- HCl [pH 7.5], 150 mM NaCl, 10%

glycerol, 1% NP-40, 10 mM sodium fluoride, 1 mM sodium pyrophosphate, 1 mM sodium orthovanadate and protease inhibitors). Cell lysates were subjected to sodium dodecyl sulfate polyacrylamide gel electrophoresis, then immunoblotted with the respective primary antibodies followed by horseradish peroxidase-conjugated secondary antibodies, and analyzed. A detail list of the antibodies used was reported previously (23).

Immunohistochemistry

Formalin-fixed, paraffin-embedded sections were stained with the respective antibodies by an avidin-biotin immunoperoxidase method. Expression of SMAD4 was evaluated as a nuclear staining, and the percentage of positively stained cells was scored as previously described (15, 24). Expression of CCL15 was interpreted as positive when $>$ 10% of the tumor cells were stained, as previously described (23, 24). We quantified the densities of $CCR1^+$ cells at the margin of lung metastases (5–9 fields ($0.1mm^2$) analyzed per one sample), as previously described (23, 24). Three researchers (TY, YI and SI) independently evaluated all immunohistochemistry samples without prior knowledge of other data. The slides with different evaluations among them

were reinterpreted at a conference to reach the consensus.

Immunofluorescence analysis

After deparaffinization of 4 μm-sliced sections, heat induced antigen retrieval was performed. The 1st antibody was applied and incubated overnight at 4 °C. After fluorescence-labeled 2nd antibody was applied (Alexa Fluor 488 anti-mouse/goat or 594 anti-rabbit), slides were mounted with a mounting medium including DAPI. Representative photos were taken by a fluorescence microscope.

Cell proliferation assay

Cells were incubated in 6-well plates (1 x 10^5 cells/well) and then cell numbers were counted at 1, 3 and 5 days later using a Countess™ Automated Cell Counter (Invitrogen, Carlsbad, CA).

In vivo xenograft studies

For experimental lung metastasis model, cancer cells (1.5 x 10^6 cells for HT29 or 3 x

10^6 cells for HCT116) were injected via tail veins of 8-week old female nude mice. For in vivo bioluminescence imaging, 3 mg of D-luciferin (VivoGlo luciferin, Promega) was injected intraperitoneally into anesthetized tumor-bearing mice 10 min before imaging. Bioluminescence from the luciferase-expressing tumor cells was monitored at days 7, 14, 21, 28 and 35 post-injection, using a Xenogen IVIS system (Xenogen Corporation, Alameda, CA). In the CCR1 antagonist-treated metastasis experiment, 3 x 10^6 cancer cells (Luc-HT29 cMyc-tag cells) were injected via tail veins of 8-week old female SCID mice. As a CCR1 antagonist, J-113863 (10 mg/kg) (TOCRIS Bioscience, Bristol, United Kingdom) was intraperitoneally administered from 1 day before tumor injection to the end of analyses (25). The animal experiment was approved by the Animal Care and Use Committee of Kyoto University.

Statistical analysis

Analyzed values are expressed as means ± standard deviation (SD). Categorical data were determined with Fisher's exact test. Continuous variables were determined with Student's *t*-test or Mann-Whitney *U* test. For factors associated with CCL15

expression, multivariate logistic regression analysis was used and factors with a *P* value of < 0.15 were included in the model. Probability of survival was analyzed by the Kaplan-Meier method using the date of pulmonary resection as the starting point. The significance of differences between subgroups was calculated using the log-rank test. Multivariate analysis of the prognostic factors was carried out using the Cox's proportional hazard regression model. Relationships between variables were determined by Pearson's correlation coefficients. All analyses were two-sided, and a *P* value with < 0.05 was considered as statistically significant. Statistical analyses were performed with the JMP Pro software, version 11.0.0 (SAS Institute Inc, NC).

Results

Loss of SMAD4 in CRC lung metastases accumulates CCR1$^+$ cells through CCL15-CCR1 chemokine axis in a mouse model

We previously reported that loss of SMAD4 causes recruitment of CCR1$^+$ myeloid cells through CCL15-CCR1 axis to promote tumor invasion and liver metastasis of CRC (23, 24). Therefore, we hypothesized that CCL15 expression may also promote lung metastasis of CRC through the CCL15-CCR1 axis.

To test this hypothesis, we first examined the role of SMAD4 in lung metastasis of CRC using a mouse model. We injected luciferase (Luc)-expressing human CRC cells into the tail veins of nude mice, and then monitored the metastasized tumor cells within the lungs by bioluminescence. A SMAD4-deficient CRC cell line, HT29, endogenously expressed high levels of CCL15, whereas over-expression of cMyc-tagged SMAD4 in these cells (Luc-HT29 cMyc-*SMAD4*) dramatically reduced CCL15 expression without affecting cell viability (Supplementary Fig. S1A and B) (23, 24). When Luc-HT29 cMyc-*SMAD4* cells were injected into nude mice through the tail veins, their lung luciferase activities were reduced compared with the controls (Fig. 1A). We dissected

lungs 35 days after injection and examined metastatic foci by bioluminescence. Although the SMAD4-deficient cells (Luc-HT29 cMyc-tag) formed foci in 38.9% of their lungs (14 of 36 lungs), the SMAD4-expressing cells (Luc-HT29 cMyc-*SMAD4*) metastasized to lungs in only 13.2% (5 of 38 lungs) (Fig. 1B; $P = 0.02$). We histologically examined the mouse lungs containing metastatic CRC cells. As anticipated, lung tumors of Luc-HT29 cMyc-tag cells expressed CCL15, whereas those with Luc-HT29 cMyc-*SMAD4* cells did not (Fig. 1C). Consistently, $CCR1^+$ cells were accumulated around the lung metastases of Luc-HT29 cMyc-tag cells, whereas few $CCR1^+$ cells accumulated around those of Luc-HT29 cMyc-*SMAD4* cells (Fig. 1C). Next, we used another CRC cell line, HCT116, in which SMAD4 was endogenously expressed (Supplementary Fig. S1C-E). In HCT116 cells engineered with stable SMAD4 knockdown (Luc-HCT116 sh*SMAD4*), sh*SMAD4* construct decreased SMAD4 expression and increased CCL15 expression, as previously reported (23). When injected into nude mice through the tail veins, Luc-HCT116 sh*SMAD4* cells formed foci in 50% of their lungs (9 of 18 lungs), while the control cells (Luc-HCT116 scramble) metastasized to lungs in only 25% (6 of 24 lungs) (Fig. 1D and E; $P = 0.12$). Histological analysis indicated that lung tumors of Luc-HCT116

sh*SMAD4* cells expressed CCL15, whereas those with Luc-HCT116 scramble cells did not (Fig. 1F). Consistently, $CCR1^+$ cells were accumulated around the lung metastases of Luc-HCT116 sh*SMAD4* cells, whereas few $CCR1^+$ cells accumulated around those of Luc-HCT116 scramble cells (Fig. 1F). Finally, we evaluated a CCR1 antagonist (J-113863) for its suppressive effect in the mouse lung metastasis model. J-113863 did not affect the proliferation rate of Luc-HT29 cMyc-tag cells *in vitro* (Supplementary Fig. S1F). We administered J-113863 (25) or the vehicle to SCID mice that were injected with Luc-HT29 cMyc-tag cells (Supplementary Fig. S1G). Luc-HT29 cMyc-tag cells do not necessarily metastasize to the lungs in nude mice (Fig. 1B), but we found they could inevitably metastasize to the lungs in SCID mice (Fig. 1G). Treatment of the host mice with 10 mg/kg of J-113863 tended to reduce the luminescence levels compared with vehicle-treated mice at day 21 (17.11 ± 18.54 vs. 5.54 ± 6.71, respectively; $P = 0.12$), although there was no apparent difference in the luminescence levels between the two groups at day 14 (Fig. 1H and Supplementary Fig. S1H). As anticipated, we verified by IHC analysis that J-113863 reduced the accumulation of $CCR1^+$ cells around the lung metastases of Luc-HT29 cMyc-tag cells (Fig. 1I). These results indicate that loss of

SMAD4 in CRC cells promotes CCL15 expression to recruit $CCR1^+$ cells, which causes metastatic colonization of tumor cells disseminated to the lungs in this mouse model.

Loss of SMAD4 is associated with CCL15 expression and $CCR1^+$ cell accumulation, which can result in lung metastasis.

In order to confirm the clinical relevance of the results from the mouse model, we next investigated expressions of SMAD4, CCL15 and CCR1 using clinical specimens of CRC lung metastases resected between 2006 and 2013 (Table 1). Of 107 lung metastases obtained from 81 patients, we found that 58% (62 of 107) was negative for SMAD4 expression, whereas 42% (45 of 107) was positive (Table 1). Immunohistochemistry indicated that CCL15 was expressed mainly at the marginal parts rather than the center of the lung metastases (Fig. 2A), and that CCL15 expression was positive in 76% (81 of 107) (Table 1), which is similar to the frequencies in primary tumors and liver metastases of CRC (23, 24). Especially, CCL15 expression was positive in 85% (53 of 62) of the SMAD4-negative metastases, whereas it was found in 62% (28 of 45) of the SMAD4-positive metastases, with a significant inverse correlation between SMAD4 and

CCL15 (odds ratio = 0.22; $P < 0.01$, Table 1).

Univariate analysis of each clinicopathological factor indicated that CCL15 expression was significantly correlated with SMAD4 expression ($P = 0.02$), and tended to be correlated with tumor location of the primary CRC ($P = 0.13$) and T factor of the primary CRC ($P = 0.14$) (Table 2). In the multivariate analysis including factors with a P value of < 0.15, only SMAD4 expression remained significantly correlated with CCL15 expression (Table 2; $P = 0.043$), showing a significant inverse correlation between CCL15 and SMAD4.

Regarding the relationship between CCL15 expression and $CCR1^+$ cell accumulation, we found that numerous $CCR1^+$ cells accumulated around the CCL15-positive CRC cells in the lung, but few around the CCL15-negative ones (Fig. 2A). We quantified the density of $CCR1^+$ cells at the periphery of lung metastases, and found that ~1.9 times more $CCR1^+$ cells around the CCL15-positive metastases than around CCL15-negative ones (12.0 ± 6.8 vs. 22.6 ± 16.0; $P < 0.01$, Table 1; Fig. 2B). These results are consistent with the CRC data for the primary tumors and liver metastases (23, 24). We also determined whether $CCR1^+$ cell density was correlated with the metastatic tumor size, and found

little correlation between them (P = 0.249; Pearson's correlation coefficients; Fig. 2C), which is different from the data of the liver metastases of CRC (23).

Expression of CCL15 in lung metastases predicts poor survival after pulmonary resection of metastatic CRC.

To evaluate the clinical outcome of CCL15 expression, we analyzed RFS of 67 CRC patients who underwent curative resection of lung metastases. The median follow-up was 32 months, and the estimated RFS rate at 3- and 5-year was 38.8% and 33.1%, respectively (Supplementary Fig. S2A-D). Statistical analyses showed that the CRC patients with CCL15-positive metastases exhibited a significantly shorter RFS than those with CCL15-negative metastases (P = 0.02, Fig. 2D). The cumulative 3-year RFS rate of CRC patients with CCL15-positive metastases was 33.0%, whereas that of those with CCL15-negative metastases was 66.0%. We previously reported that CCL15 expression on primary tumors or liver metastases of CRC is correlated with patients' RFS (23, 24). The present results are consistent with our previous studies, supporting that SMAD4-deficient CRC can worsen patients' survival through the CCL15-CCR1

chemokine axis to accumulate $CCR1^+$ cells in the tumor microenvironment. We also analyzed overall survival (OS) of 81 patients who underwent pulmonary resection (Supplementary Fig. S3A), and found that CCL15 expression tended to correlate with shorter OS although without a significant difference ($P = 0.14$, Supplementary Fig. S3B).

In CRC patients who underwent complete pulmonary resection in a large-scale retrospective analysis, it has been recently reported that the number of pulmonary metastatic lesions, their distribution, the tumor size, the serum carcinoembryonic antigen (CEA) level prior to pulmonary resection, the disease-free interval, and the lymph node metastases of primary CRC are independent prognostic factors for prognosis (5-8). Therefore, we also analyzed the effect of CCL15 expression in conjunction with these factors in this study. According to a univariate analysis, T stage of primary CRC, N stage of primary CRC, CEA level prior to pulmonary resection, and CCL15 expression in lung metastases were significant predictors of shorter RFS (Table 3; Supplementary Fig. S2B-D). In the multivariate analysis including these variables, CCL15 expression in lung metastases was the only parameter that remained significant for predicting shorter RFS (Table 3; hazard ratio [HR], 2.53; 95% confidence interval [CI], 1.11–6.67; $P = 0.026$).

Characterization of CCR1$^+$ cells accumulated around lung metastases of CRC

We previously reported that CCR1$^+$ cells accumulating around the invasion front of primary CRC were of the MDSC phenotype, and that most of these CCR1$^+$ MDSCs were of the granulocytic-MDSC lineage (24). In order to determine whether the CCR1$^+$ cells accumulating around lung metastases of CRC were of the same phenotype as those in the primary CRC, we performed double immunofluorescence staining with several cell-type specific markers. The majority of these CCR1$^+$ cells were positive for MPO, CD11b, CD15 and CD16, while they were negative for HLA-DR, CD33, CD3, CD8, CD14, CD68 and α-SMA (Fig. 3A-F and Supplementary Fig. S4A-E), suggesting that they were of the TAN phenotype (CD11b$^+$, CD33$^-$, HLA-DR$^-$, CD15$^+$ and CD16$^+$). TANs are characterized by having immunosuppressive (by producing ARG1) and angiogenic (by producing MMP) functions (12, 13, 14). Consistently, we confirmed that these CCR1$^+$ cells expressed ARG1 in addition to MMP9 (Fig. 3G and H), and that a subpopulation of these CCR1$^+$ cells was positive for CXCR2 (Supplementary Fig. S4F), a major chemokine receptor expressed on TAN (12). Moreover, we also observed that only a

minor fraction of $CCR1^+$ cells were positive for CD11b, CD33 and CD15 with negative HLA-DR (Supplementary Fig. S5A-D), suggesting that they were of the granulocytic-MDSC lineage.

Discussion

It has been shown that various types of myeloid cells promote tumor progression by immune suppression as well as by facilitating cell growth, migration and angiogenesis. These cells include TAMs, MDSCs and more recently TANs (12, 13, 14). TAMs, the best-characterized among them, are divided into two populations: M2 macrophages that promote tumorigenesis and M1 macrophages that are antitumorigenic. MDSCs constitute a heterogeneous population of immature myeloid cells that are increased in cancer, inflammation and infection (26). Human MDSCs comprise two subpopulations; monocytic-MDSCs (HLA-DR$^-$, CD11b$^+$, CD33$^+$ and CD14$^+$) and granulocytic-MDSCs HLA-DR$^-$, CD11b$^+$, CD33$^+$ and CD15$^+$). On the other hand, the presence and functional characteristics of TANs may have been underestimated and therefore need reappraisal. As defined with M1 and M2 TAMs, TANs also have differential states of activation/differentiation: N1 neutrophils are antitumorigenic, whereas N2 neutrophils display protumorigenic properties (27, 28). It has been reported that, in a mouse lung cancer model, TGF-β is a major cytokine within tumors that defines the TAN phenotype and skews differentiation toward the N2 phenotype (27). We previously reported that

CCL15 expression by loss of SMAD4 in cancer cells helps recruitment of $CCR1^+$ MDSCs ($CD11b^+$, $CD33^+$, and $HLA\text{-}DR^-$) at the invasion front of primary CRC (24). In this study of the lung metastases of CRC, we have verified that CCL15 expression was significantly correlated with loss of SMAD4 (Table 1), and that CCL15-positive metastases recruited more numbers of $CCR1^+$ cells than CCL15-negative metastases did (Table 1; Fig. 2B). $CCR1^+$ cells accumulating around lung metastases were positive for MPO, CD11b, CD15 and CD16 (Fig. 3A, B, E, and F), while they were negative for HLA-DR, CD3, CD8 and α-SMA (Fig. 3D, and Supplementary Fig S4A, B and D), suggesting their myeloid origin rather than lymphoid or fibroblastic origins. Contrary to our anticipation, most of these $CCR1^+$ cells expressed mature myeloid cell markers (positive MPO and negative CD33) (Fig. 3A and C), and granulocyte-lineage markers (MPO, CD15 and CD16) (Fig. 3A, E and F), while they lacked monocyte-lineage markers (CD68 and CD14) (Supplementary Fig. S4C and E). These cells may contribute to the development of tumor microenvironment through production of MMP9 and ARG1 (Fig. 3G and H). We also found that only a minor fraction of $CCR1^+$ cells were positive for CD11b, CD33 and CD15 with negative HLA-DR (Supplementary Fig. S5A-D). Taken together, these results

indicate that CCR1$^+$ cells accumulating around lung metastases of CRC are composed mainly of the TAN and only partially of the granulocytic-MDSC, which may suggest these myeloid cell subsets are specific to the tumor and organ. Regarding the CCR1$^+$ cells accumulating around CRC liver metastases, we previously reported that these CCR1$^+$ cells were positive for both CD11b and MPO (23). In this study, we further characterized these CCR1$^+$ cells using double immunofluorescence staining, and found that most of CCR1$^+$ cells were positive for MPO, CD11b, CD15, CD16, ARG1 and MMP9 while they were negative for HLA-DR and CD33 (Supplementary Fig. S6A-H), which suggests that they are composed mainly of TAN. Regarding the relationship between TANs and MDSCs, it has been suggested that MDSCs can enter tumors and differentiate to mature TAMs or TANs (29). It remains to be determined whether the neutrophils within the tumors are derived from granulocytic-MDSCs or whether they are blood-derived neutrophils converted to the N2 phenotype by the tumor environment (e.g., high local concentration of TGF-β). To further characterize the cell lineage and the functions of these myeloid cells, our next step would be to isolate viable tumor-associated CCR1$^+$ myeloid cells from the tumor tissues by fluorescence activated cell sorting. Several

studies show that an elevated neutrophil count in the peripheral blood (i.e., a high neutrophil-to-lymphocyte ratio (NLR)) is associated with poor clinical outcomes in several types of cancer including CRC (30), emphasizing the importance and relevance of neutrophils in cancer biology.

Chemokine CCL15, a member of the CC chemokine family and constitutively expressed in the gut and liver, was cloned and partially characterized (31). CCL15 plays an important role in the development of inflammation and allergic diseases (32, 33, 34), and binds mainly to CCR1 as a chemoattractant for monocytes, neutrophils, lymphocytes and dendritic cells (35). Accumulating evidence has suggested that CCL15 has a crucial role in the progression of several types of cancer including CRC, hepatocellular carcinoma (HCC), and lung cancer (23, 24, 36-39). We previously showed that SMAD4 binds directly to the promoter region of human *CCL15* gene to negatively regulate its expression, and that CCL15 expression is inversely correlated with SMAD4 expression in clinical specimens of human primary CRC and its liver metastasis (23, 24). In the lung metastases of CRC, we have determined here that there is a significant

inverse correlation between CCL15 and SMAD4 levels by immunohistochemical analysis of 107 clinical samples (Table 1 and 2). Expression of SMAD4 was lost in 58% (62 of 107), whereas that of CCL15 was found in 76% (81 of 107). The difference of ~20% between these frequencies suggests that factors other than SMAD4 can also contribute to CCL15 expression. In fact, the promoter of *CCL15* contains multiple potential binding sites for transcription factors involved in the immune system and inflammation, although the functionality of these regions are yet to be investigated experimentally (35). It has been reported that CCL15 is the most significant serum markers associated with short survival in early-stage (i.e., Stage I/II) lung cancer (38). In HCC, CCL15 is one of the independent predictors of shorter OS as well as TNM stage (39). Our previous reports show that CCL15 is associated with a shorter RFS in liver metastasis and Stage I/II primary CRC (23, 24). In this study, we have also demonstrated that patients with CCL15-positive lung metastases show a significantly shorter RFS than those with CCL15-negative ones ($P = 0.02$, Fig. 2D). It is worth noting that a multivariate analysis has indicated that CCL15 expression is an independent predictor of shorter RFS ($P = 0.026$, Table 3), although further studies with a large multi-institutional cohort are

required. Taken together, CCL15 expression within tumors may be associated with poor clinical outcomes in several types of cancer.

Chemokines have overlapping actions, and their activities can be altered by proteolytic degradation. Therefore, effective targeting of chemokine pathways can require high levels of receptor occupancy throughout treatment. In mouse models, tumor invasion and metastasis of CRC were suppressed by inhibiting CCL15-CCR1 signaling with a CCR1 inhibitor, genetic knockdown of *CCL15* gene, or *CCR1* knockout mice (20, 21, 23, 24, 40). In addition, it has been reported recently that activation of CCL2/CCR2 axis prompts TAMs to secrete another chemokine CCL3, which in turn activates its receptor CCR1 in TAMs and promotes lung metastatic seeding of breast cancer in a mouse model (41). These results suggest that inhibition of CCR1 may have a therapeutic impact on metastatic progression of certain types of cancer, including CRC and breast cancer. A number of CCR1 inhibitors have already been used in phase I/II clinical trials for rheumatoid arthritis, chronic obstructive pulmonary disease and multiple sclerosis (42, 43). Thus, it would be worthwhile to test CCR1 inhibitors to prevent cancer metastasis,

because they have been already cleared for safety concerns.

Authors' Contributions

Conception and design: K. Kawada, Y. Itatani, Y. Sakai,

Development of methodology: K. Kawada,

Acquisition of data: T. Yamamoto, S. Inamoto, Y. Itatani, M. Iwamoto,

Analysis and interpretation of data: T. Yamamoto, S. Inamoto, K. Kawada,

Writing, review, and/or revision of the manuscript: K. Kawada, Y. Itatani, T. Yamamoto, H. Hirai, S. Hasegawa, M. Mark. Taketo,

Administrative, technical, or material support: M. Iwamoto, E. Miyamoto, T. f Chen-Yoshikawa, H. Hirai, H. Date,

Study supervision: M. Mark. Taketo, Y. Sakai

References

1. Mitry E, Guiu B, Cosconea S, Jooste V, Faivre J, Bouvier AM. Epidemiology, management and prognosis of colorectal cancer with lung metastases: a 30-year population-based study. Gut 2010;59:1383-8.
2. Kobayashi H, Mochizuki H, Sugihara K, Morita T, Kotake K, Teramoto T, et al. Characteristics of recurrence and surveillance tools after curative resection for colorectal cancer: a multicenter study. Surgery 2007;141:67-75.
3. Watanabe T, Itabashi M, Shimada Y, Tanaka S, Ito Y, Ajioka Y, et al. Japanese Society for Cancer of the Colon and Rectum (JSCCR) Guidelines 2014 for treatment of colorectal cancer. Int J Clin Oncol 2015;20:207-39.
4. Chen F, Sakai H, Miyahara R, Bando T, Okubo K, Date H. Repeat resection of pulmonary metastasis is beneficial for patients with colorectal carcinoma. World J Surg. 2010;34:2373-8.
5. Iida T, Nomori H, Shiba M, Nakajima J, Okumura S, Horio H, et al. Prognostic factors after pulmonary metastasectomy for colorectal cancer and rationale for

determining surgical indications: a retrospective analysis. Ann Surg 2013;257:1059-64.

6. Hirosawa T, Itabashi M, Ohnuki T, Yamaguchi N, Sugihara K, Kameoka S; Japanese Society for Cancer of the Colon and Rectum (JSCCR) Study Group for Pulmonary Metastases from Colorectal Cancer. Prognostic factors in patients undergoing complete resection of pulmonary metastases of colorectal cancer: a multi-institutional cumulative follow-up study. Surg Today 2013;43:494-9.
7. Suzuki H, Kiyoshima M, Kitahara M, Asato Y, Amemiya R. Long-term outcomes after surgical resection of pulmonary metastases from colorectal cancer. Ann Thorac Surg 2015;99:435-40.
8. Hirosawa T, Itabashi M, Ohnuki T, Yamaguchi N, Sugihara K, Kameoka S; Japanese Society for Cancer of the Colon and Rectum (JSCCR) Study Group for Pulmonary Metastases from Colorectal Cancer. Proposal of a new prognostic staging system for pulmonary metastases from colorectal cancer. Surg Today 2015;45:576-84.

9. Chen F, Hanaoka N, Sato K, Fujinaga T, Sonobe M, Shoji T, et al. Prognostic factors of pulmonary metastasectomy for colorectal carcinomas. World J Surg. 2009;33:505-11.
10. Kaplan RN, Riba RD, Zacharoulis S, Bramley AH, Vincent L, Costa C, et al. VEGFR1-positive haematopoietic bone marrow progenitors initiate the pre-metastatic niche. Nature 2005;438:820-7.
11. Yang L, Huang J, Ren X, Gorska AE, Chytil A, Aakre M, et al. Abrogation of TGFβ signaling in mammary carcinomas recruits Gr-1+CD11b+ myeloid cells that promote metastasis. Cancer Cell 2008;13:23-35.
12. Murdoch C, Muthana M, Coffelt SB, Lewis CE. The role of myeloid cells in the promotion of tumour angiogenesis. Nat Rev Cancer 2008;8:618-31.
13. Gabrilovich DI, Ostrand-Rosenberg S, Bronte V. Coordinated regulation of myeloid cells by tumours. Nat Rev Immunol 2012;12:253-68.
14. Kitamura T, Qian BZ, Pollard JW. Immune cell promotion of metastasis. Nat Rev Immunol 2015;15:73-86.

15. Salovaara R, Roth S, Loukola A, Launonen V, Sistonen P, Avizienyte E, et al. Frequent loss of SMAD4/DPC4 protein in colorectal cancers. Gut 2002;51:56-9.
16. Roth AD, Delorenzi M, Tejpar S, Yan P, Klingbiel D, Fiocca R, et al. Integrated analysis of molecular and clinical prognostic factors in stage II/III colon cancer. J Natl Cancer Inst 2012;104:1635-46.
17. Alazzouzi H, Alhopuro P, Salovaara R, Sammalkorpi H, Järvinen H, Mecklin JP, et al. Hemminki A, Schwartz S, Aaltonen LA, Arango D. SMAD4 as a prognostic marker in colorectal cancer. Clin Cancer Res 2005;11:2606-11.
18. Voorneveld PW, Jacobs RJ, Kodach LL, Hardwick JC. A Meta-Analysis of SMAD4 Immunohistochemistry as a Prognostic Marker in Colorectal Cancer. Transl Oncol 2015;8:18-24.
19. Takaku K, Oshima M, Miyoshi H, Matsui M, Seldin MF, Taketo MM. Intestinal tumorigenesis in compound mutant mice of both Dpc4 (Smad4) and Apc genes. Cell 1998;92:645-56.

20. Kitamura T, Kometani K, Hashida H, Matsunaga A, Miyoshi H, Hosogi H, et al. SMAD4-deficient intestinal tumors recruit CCR1+ myeloid cells that promote invasion. Nat Genet 2007;39:467–475.
21. Kitamura T, Fujishita T, Loetscher P, Revesz L, Hashida H, Kizaka-Kondoh S, et al. Inactivation of chemokine (C-C motif) receptor 1 (CCR1) suppresses colon cancer liver metastasis by blocking accumulation of immature myeloid cells in a mouse model. Proc Natl Acad Sci USA 2010;107:13063–13068.
22. Hirai H, Fujishita T, Kurimoto K, Miyachi H, Kitano S, Inamoto S, et al. CCR1-mediated accumulation of myeloid cells in the liver microenvironment promoting mouse colon cancer metastasis. Clin Exp Metastasis 2014;31:977-89.
23. Itatani Y, Kawada K, Fujishita T, Kakizaki F, Hirai H, Matsumoto T, et al. Loss of SMAD4 from colorectal cancer cells promotes CCL15 expression to recruit CCR1+ myeloid cells and facilitate liver metastasis. Gastroenterology 2013;145:1064-1075.
24. Inamoto S, Itatani Y, Yamamoto T, Minamiguchi S, Hirai H, Iwamoto M, et al. Loss of SMAD4 Promotes Colorectal Cancer Progression by Accumulation of

Myeloid-Derived Suppressor Cells through the CCL15-CCR1 Chemokine Axis. Clin Cancer Res 2016;22:492-501.

25. Amat M, Benjamim CF, Williams LM, Prats N, Terricabras E, Beleta J, et al. Pharmacological blockade of CCR1 ameliorates murine arthritis and alters cytokine networks in vivo. Br J Pharmacol 2006;149:666-675.

26. Gabrilovich DI, Nagaraj S. Myeloid-derived suppressor cells as regulators of the immune system. Nat Rev Immunol 2009;9:162-74.

27. Fridlender ZG, Sun J, Kim S, Kapoor V, Cheng G, Ling L, et al. Polarization of tumor-associated neutrophil phenotype by TGF-beta: "N1" versus "N2" TAN. Cancer Cell 2009;16:183-94.

28. Mantovani A, Cassatella MA, Costantini C, Jaillon S. Neutrophils in the activation and regulation of innate and adaptive immunity. Nat Rev Immunol 2011;11:519-31.

29. Kusmartsev S, Nagaraj S, Gabrilovich DI. Tumor-associated CD8+ T cell tolerance induced by bone marrow-derived immature myeloid cells. J Immunol 2005;175:4583-92.

30. Guthrie GJ, Charles KA, Roxburgh CS, Horgan PG, McMillan DC, Clarke SJ. The systemic inflammation-based neutrophil-lymphocyte ratio: experience in patients with cancer. Crit Rev Oncol Hematol 2013 ;88:218-30.

31. Pardigol A, Forssmann U, Zucht HD, Loetscher P, Schulz-Knappe P, Baggiolini M, et al. HCC-2, a human chemokine: gene structure, expression pattern, and biological activity. Proc Natl Acad Sci U S A 1998;95:6308-13.

32. Berahovich RD, Miao Z, Wang Y, Premack B, Howard MC, Schall TJ. Proteolytic activation of alternative CCR1 ligands in inflammation. J Immunol 2005;174:7341-51.

33. Joubert P, Lajoie-Kadoch S, Wellemans V, Létuvé S, Tulic MK, Halayko AJ, et al. Expression and regulation of CCL15 by human airway smooth muscle cells. Clin Exp Allergy 2012;42:85-94.

34. Park KH, Lee TH, Kim CW, Kim J. Enhancement of CCL15 expression and monocyte adhesion to endothelial cells (ECs) after hypoxia/reoxygenation and induction of ICAM-1 expression by CCL15 via the JAK2/STAT3 pathway in ECs. J Immunol 2013;190:6550-8.

35. Forssmann U, Magert HJ, Adermann K, Escher SE, Forssmann WG. Hemofiltrate CC chemokines with unique biochemical proterties: HCC-1/CCL14a and HCC2/CCL15. J Leukoc Biol 2001;70;357-366.

36. Reckamp KL, Gardner BK, Figlin RA, Elashoff D, Krysan K, Dohadwala M, et al. Tumor response to combination celecoxib and erlotinib therapy in non-small cell lung cancer is associated with a low baseline matrix metalloproteinase-9 and a decline in serum-soluble E-cadherin. J Thorac Oncol 2008;3:117-24.

37. Li Y, Wu J, Zhang W, Zhang N, Guo H. Identification of serum CCL15 in hepatocellular carcinoma. Br J Cancer 2013;108:99-106.

38. Bodelon C, Polley MY, Kemp TJ, Pesatori AC, McShane LM, Caporaso NE, et al. Circulating levels of immune and inflammatory markers and long versus short survival in early-stage lung cancer. Ann Oncol 2013;24:2073-9.

39. Li Y, Yu HP, Zhang P. CCL15 overexpression predicts poor prognosis for hepatocellular carcinoma. Hepatol Int. 2015 Dec 7. [Epub ahead of print]

40. Rodero MP, Auvynet C, Poupel L, Combadière B, Combadière C. Control of both myeloid cell infiltration and angiogenesis by CCR1 promotes liver cancer metastasis development in mice. Neoplasia 2013;15:641-8.

41. Kitamura T, Qian BZ, Soong D, Cassetta L, Noy R, Sugano G, et al. CCL2-induced chemokine cascade promotes breast cancer metastasis by enhancing retention of metastasis-associated macrophages. J Exp Med 2015;212:1043-59.

42. Gladue RP, Brown MF, Zwillich SH. CCR1 antagonists: what have we learned from clinical trials. Curr Top Med Chem 2010;10:1268-77.

43. Szekanecz Z, Koch AE. Successes and failures of chemokine-pathway targeting in rheumatoid arthritis. Nat Rev Rheumatol. 2016;12:5-13.

Table1 : Univariate analysis of factors associated with CCL15expression

Factors	CCL15 negative (n = 26)	CCL15 positive (n = 81)	*P*-value
tumor size (mm)	17.4 ± 15.2	14.5 ± 10.7	0.68
SMAD4 expression			
negative	9	53	
positive	17	28	< 0.01
CCR1-positive cell count	12.0 ± 6.8	22.6 ± 16.0	< 0.01

Table2 : Univariate analysis of clinico-pathological factors for CCL15 expression

	Univariate analysis			Multivariate analysis		
Variables	CCL15 negative	CCL15 positive	*P*-value	OR	95%CI	*P*-value
Age						
< 60	8	15				
60 ≤	12	46	0.25			
Sex						
Male	12	36				
Female	8	25	1.00			
Location						
Colon	7	34				
Rectum	13	27	0.13	1.73	0.56 - 5.56	0.34
Histology						
tub1 / tub2	14	42				
por / sig / muci	1	5	1.00			
T factor						
1 / 2	3	3				
3 / 4	15	56	0.14	0.47	0.07 - 3.09	0.42
N factor						
Negative	7	22				
Positive	12	38	1.00			
M factor						
Negative	12	40				
Positive	7	20	0.79			
H factor						
Negative	15	49				
Positive	4	11	0.75			
venous invasion						
Negative	5	11				
Positive	9	39	0.31			
lymphatic invasion						
Negative	6	29				
Positive	9	22	0.38			
Prior chemotherapy						
Negative	9	34				
Positive	11	27	0.45			
Neoadjuvant treatment						
Negative	13	43				
Positive	7	18	0.78			
Timing						
Synchronous	3	10				
Metachronous	17	51	1.00			
Other metastases						
Negative	9	25				

Positive	11	35	0.80			
Tumor size						
< 20mm	15	41				
20mm≤	5	17	0.78			
Number of metastases						
1 / 2	19	57				
3 ≤	1	4	1.00			
Hilar / Mediastinal LN						
Negative	20	57				
Positive	0	4	0.57			
Disease free interval						
< 2years	8	21				
2years ≤	12	40	0.79			
CEA (ng/mL)						
< 5.0	15	45				
5.0 ≤	5	15	1.00			
CA19-9 (U/mL)						
< 37	8	31				
37 ≤	1	5	1.00			
NLR						
< 3.0	16	43				
3.0 ≤	4	18	0.56			
SMAD4 expression						
Negative	7	40				
Positive	13	21	0.02	3.26	1.04 - 10.97	0.043

Table3 : Univariate and multivariate analysis of clinico-pathological factors for relapse free survival

		Univariate analysis			Multivariate analysis		
variables	N	HR	95%CI	*P*-value	HR	95%CI	*P*-value
Age							
< 60	20						
60 ≤	47	1.03	0.54 - 2.10	0.93			
Sex							
Male	37						
Female	30	0.66	0.34 - 1.24	0.20			
Location							
Colon	34						
Rectum	33	0.82	0.44 - 1.52	0.52			
Histology							
tub1 / tub2	46						
por / sig / muci	5	0.71	0.11 - 2.35	0.62			
T factor							
1 / 2	6						
3 / 4	58	3.30	1.00 - 20.3	0.049	2.18	0.59 - 14.36	0.27
N factor							
Negative	23						
Positive	43	2.03	1.04 - 4.25	0.038	0.81	0.26 - 3.52	0.75
M factor							
Negative	44						
Positive	22	1.83	0.96 - 3.43	0.07			
H factor							
Negative	52						
Positive	14	1.54	0.73 - 3.01	0.24			
venous invasion							
Negative	11						
Positive	43	0.98	0.45 - 2.45	0.96			
lymphatic invasion							
Negative	28						
Positive	27	1.31	0.67 - 2.59	0.44			
Prior chemotherapy							
Negative	37						
Positive	30	0.98	0.52 - 1.81	0.95			
Neoadjuvant treatment							
Negative	50						
Positive	17	1.49	0.73 - 2.85	0.26			
Timing							
Synchronous	12						
Metachronous	55	0.70	0.35 - 1.50	0.34			
Other metastases							
Negative	31						
Positive	36	1.53	0.83 - 2.91	0.18			

Tumor size							
< 20mm	48						
20mm ≤	17	0.95	0.44 - 1.89	0.90			
Number of metastases							
1 / 2	63						
3 ≤	4	0.83	0.14 - 2.72	0.79			
Distribution							
unilateral	57						
bilateral	10	0.94	0.32 - 2.20	0.90			
Hilar/Mediastinal LN							
Negative	63						
Positive	4	1.77	0.43 - 4.91	0.38			
Disease free interval							
< 2years	25						
2years ≤	42	0.94	0.51 - 1.78	0.84			
CEA (ng/mL)							
< 5.0	50						
5.0 ≤	16	2.07	1.03 - 3.94	0.041	1.97	0.90 - 4.14	0.09
CA19-9 (U/mL)							
< 37	32						
37 ≤	5	3.17	0.87 - 9.47	0.08			
NLR							
< 3.0	48						
3.0 ≤	19	1.08	0.53 - 2.08	0.82			
CCL15							
Negative	15						
Positive	52	2.58	1.19 - 6.47	0.015	2.54	1.11 - 6.67	0.026
SMAD4							
Negative	37						
Positive	30	0.63	0.33 - 1.17	0.15			

Figure legends

Figure 1. Mouse xenograft model of CRC lung metastasis.

A, In vivo bioluminescence images of nude mice injected with Luc-HT29 cells (left) and their lungs at 35 days post-injection (right). B, Metastasis frequencies of HT29 clones to lungs at 35 days post-injection. Metastasis frequencies based on the numbers of lungs or the number of mice were shown (Fisher's exact test; P = 0.02 and 0.09, respectively). Note that each mouse has right and left lungs. C, Immunohistochemistry analyses of mouse lung with metastatic foci. Note that SMAD4 of cMyc-*SMAD4* cells is expressed as a nuclear staining. Scale bar, 100 μm. D, Histological analyses of mouse lung with metastatic foci. Scale bar, 100 μm. E, Metastasis frequencies of HCT116 clones to lungs at 28 days post-injection. Metastasis frequencies based on the numbers of lungs or the number of mice were shown (Fisher's exact test; P = 0.12 and 0.39, respectively). F, Immunohistochemistry analyses of mouse lung with metastatic foci. Note that SMAD4 of scramble cells is expressed as a nuclear staining. Scale bar, 100 μm. G, *In vivo* bioluminescence images of SCID mice injected with Luc-HT29 cells (left) and their lungs at 21 days post-injection (right). H, Relative quantification of the lung metastatic lesions

(photon counts) in SCID mice treated with vehicle or J113863 at 10 mg/kg. Each triangle represents an individual mouse. Each photon count at day 14 and 21 was normalized to that at day 7. Horizontal lines show the means of representative groups (Student *t* test; *P* = 0.12 at day 21). *n* = 6-8 mice in each group. I, Immunohistochemistry analyses of lung metastases of mice treated with vehicle or J-113863. T, Tumor, Scale bar, 100 μm.

Figure 2. Correlation of SMAD4 loss and expression of CCL15 and CCR1 in clinical specimens of CRC lung metastases.

A, Haematoxylin and eosin staining (H&E) and immunohistochemical detection of SMAD4, CCL15 and CCR1 in lung metastases. Upper and lower panels show serial sections of representative SMAD4-deficient and SMAD4-expressing CRC, respectively. Note that SMAD4 of cancer cells is expressed as a nuclear staining. Scale bar, 100 μm. B, Quantification of the $CCR1^+$ cell density in CRC lung metastases with and without CCL15 expression (*n* = 26 and 81, respectively). *, *P* < 0.01; Mann-Whitney *U* test; horizontal bands show the means. C, Scatter plot of metastatic tumor size and $CCR1^+$ cell accumulation. The relationship was evaluated by the Pearson's correlation

coefficient (r; correlation coefficient). D, Effects of CCL15 expression on RFS in CRC patients who underwent curative pulmonary resection (Kaplan-Meier estimates).

Figure 3. Characterization of CCR1^{+} cells in the tumor microenvironment of CRC lung metastases.

Simultaneous immunofluorescence staining for CCR1 (red) and MPO (A), CD11b (B), CD33 (C), HLA-DR (D), CD15 (E), CD16 (F), ARG1 (G), or MMP9 (H) (green). Scale bar, 20 μm.

Figure 1

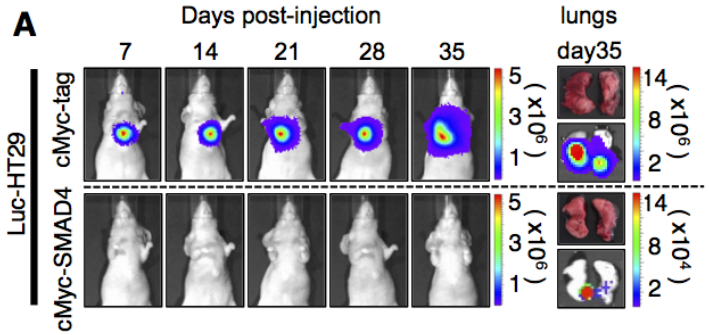

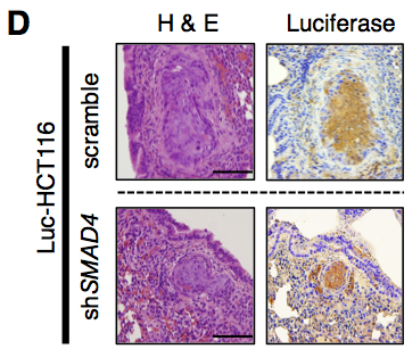

B

Luc-HT29

	cMyc-tag n = 36 lungs (18 mice)	cMyc-SMAD4 n = 38 lungs (19 mice)
metastasis		
positive	14 (9)	5 (4)
negative	22 (9)	33 (15)

P = 0.02 (*P* = 0.09)

E

Luc-HCT116

	scramble n = 24 lungs (12 mice)	sh*SMAD4* n = 18 lungs (9 mice)
metastasis		
positive	6 (5)	9 (6)
negative	18 (7)	9 (3)

P = 0.12 (*P* = 0.39)

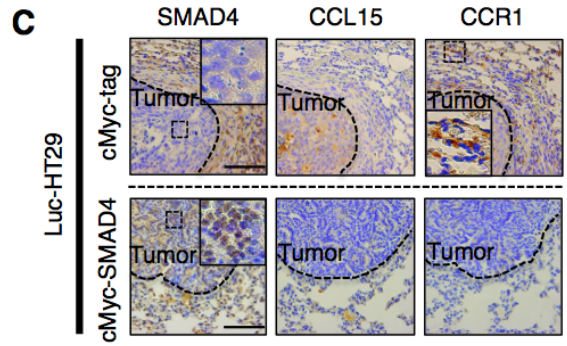

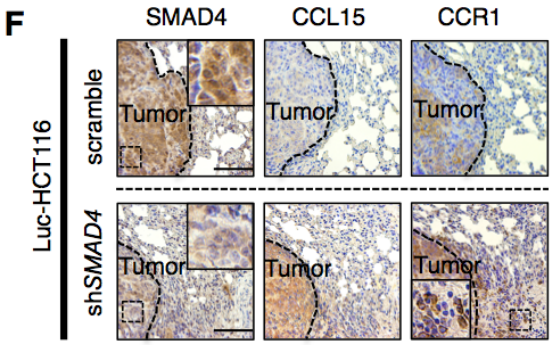

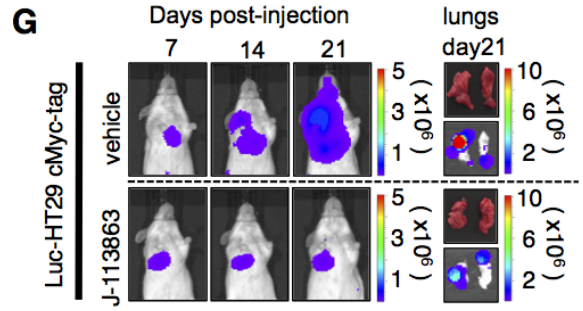

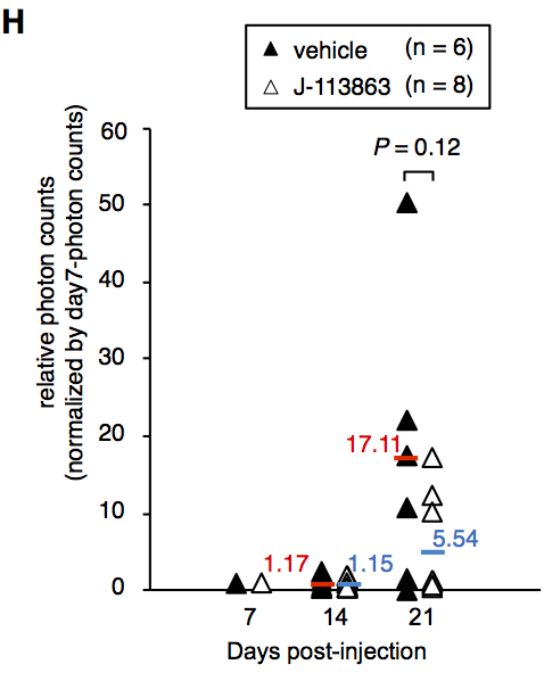

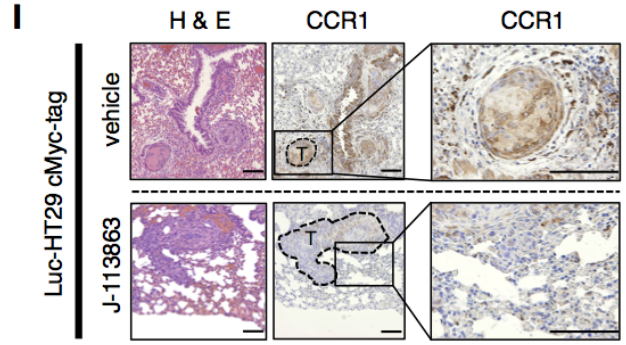

Figure 2

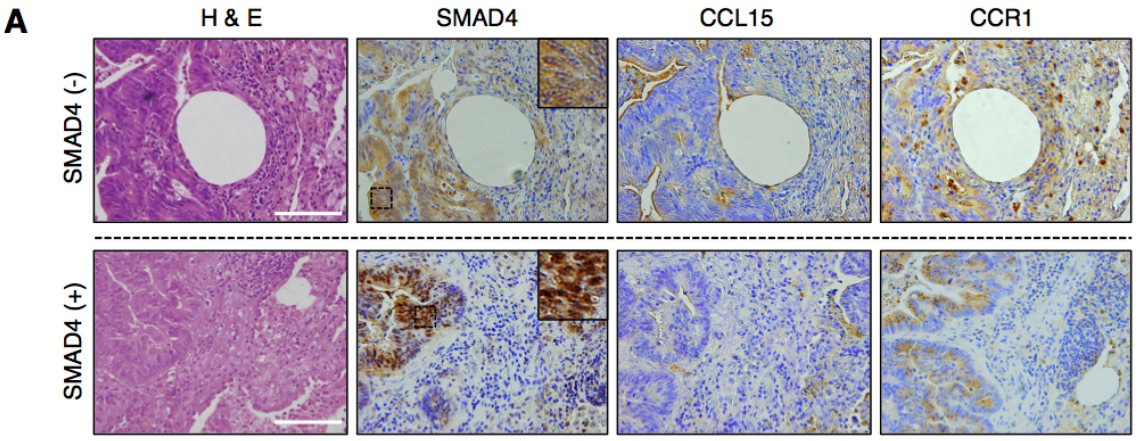

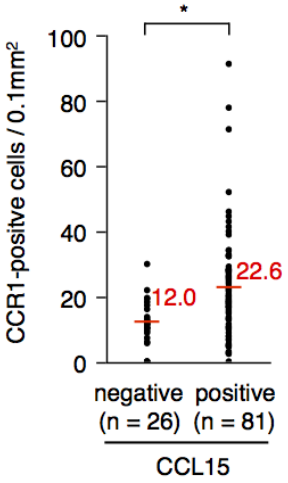

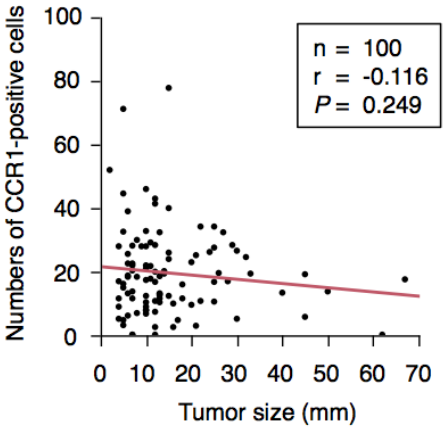

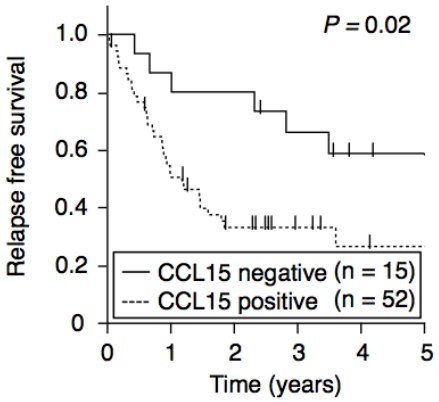

No. of patients

CCL15 negative	15	13	12	9	6	5
CCL15 positive	52	27	14	7	4	3

Figure 3

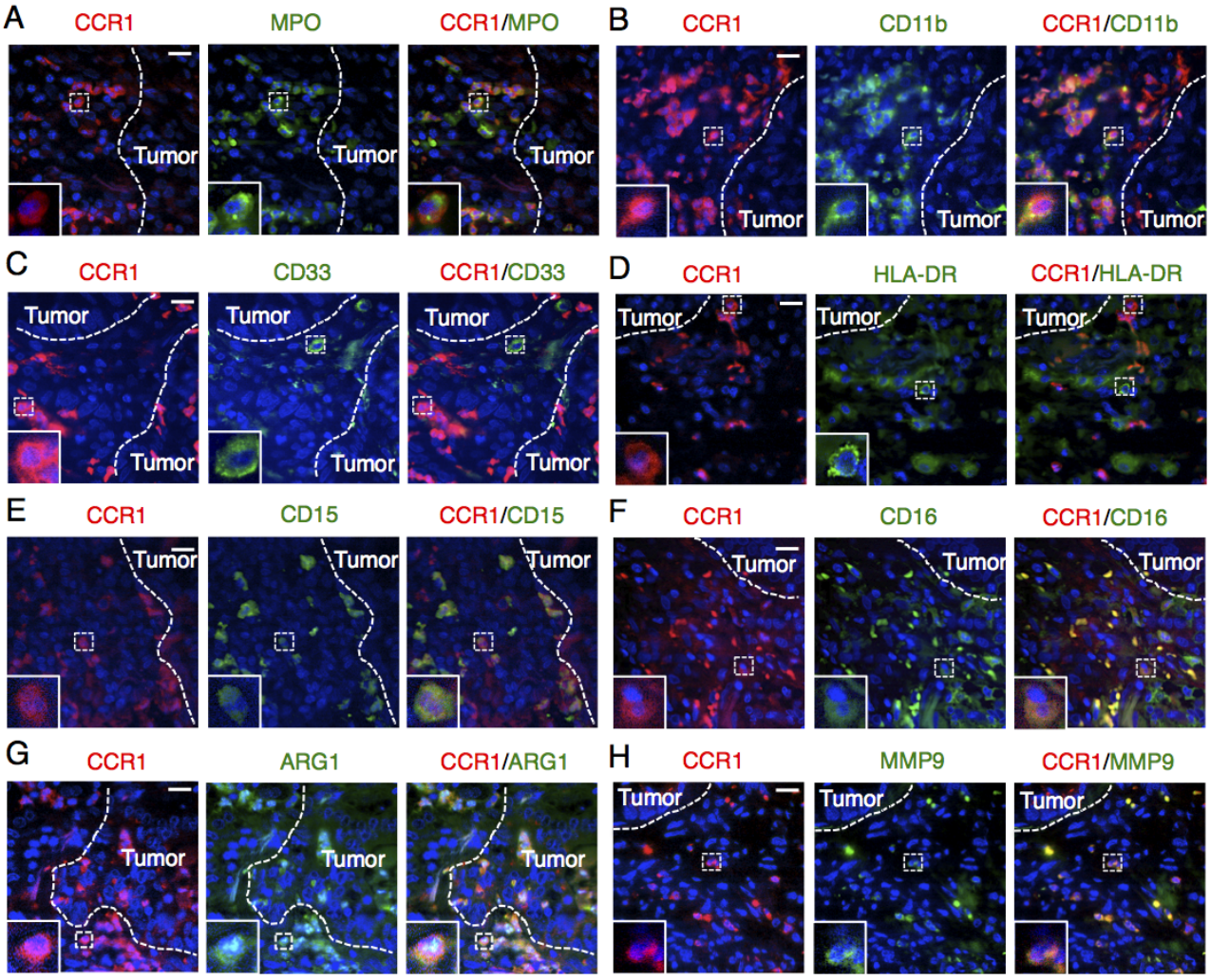
A
CCR1
MPO
CCR1/MPO
B
CCR1
CD11b
CCR1/CD11b
C
CCR1
CD33
CCR1/CD33
D
CCR1
HLA-DR
CCR1/HLA-DR
E
CCR1
CD15
CCR1/CD15
F
CCR1
CD16
CCR1/CD16
G
CCR1
ARG1
CCR1/ARG1
H
CCR1
MMP9
CCR1/MMP9
Tumor

ARTICLE INFORMATION

DOI
http://dx.doi.org/10.1158/1078-0432.CCR-16-0520

PubMed
27492974

Published By
American Association for Cancer Research

Print ISSN
1078-0432

Online ISSN
1557-3265

History
Received February 27, 2016.
Revision received July 1, 2016.
Accepted July 22, 2016.
Published first August 4, 2016.

AUTHOR INFORMATION

Takamasa Yamamoto[1], Kenji Kawada[1,*], Yoshiro Itatani[1], Susumu Inamoto[1], Ryosuke Okamura[1], Masayoshi Iwamoto[1], Ei Miyamoto[2], Toyofumi F Chen-Yoshikawa[2], Hideyo Hirai[3], Suguru Hasegawa[1], Hiroshi Date[4], Makoto Mark Taketo[5], and Yoshiharu Sakai[1]

[1]Surgery, Graduate School of Medicine, Kyoto University
[2]Thoracic surgery, Graduate School of Medicine, Kyoto University
[3]Department of Transfusion Medicine and Cell Therapy, Kyoto University Hospital
[4]Department of Thoracic Surgery, Kyoto University
[5]Pharmacology, Graduate School of Medicine, Kyoto University

↵* **Corresponding Author:**
Kenji Kawada, Surgery, Graduate School of Medicine, Kyoto University, 54 Shogoin-Kawahara-cho, Sakyo-ku, Kyoto, 606-8507, Japan. E-mail: kkawada@kuhp.kyoto-u.ac.jp

Supplementary Figure legends

Supplementary Figure S1.

A and B, Western blot analysis of SMAD4 (A) and quantitative RT-PCR analysis of *CCL15* mRNA (B) in luciferase-expressing HT29 cells where *SMAD4* was stably overexpressed (Luc-HT29 cMyc-*SMAD4*). *, $P < 0.05$. C and D, Western blot analysis of SMAD proteins (SMAD4, SMAD5, SMAD2/3 and SMAD1) (C) and quantitative RT-PCR analysis of *CCL15* mRNA (D) in HT29 and HCT116 cells. E, Immunohistochemistry analyses of mouse lung with metastatic foci of HT29 and HCT116 cells. Scale bar, 100μm. F, Cell proliferation *in vitro* of Luc-HT29 cMyc-tag cells treated with DMSO (control) or J-113863 (0.01μM, 0.1μM, 1μM, and 10μM). G, Experimental schedule of treatment with vehicle or J-113863. H, Relative quantification of the lung metastatic lesions (photon counts) in SCID mice treated with vehicle or J-113863 at 10 mg/kg. Each photon count at day 14 and 21 was normalized to that at day 7.

Supplementary Figure S2.

A, Kaplan-Meier curves of RFS in CRC patients after curative pulmonary resection (Kaplan-Meier estimates). B, Effect of T factor of primary CRC on RFS after curative

pulmonary resection (Kaplan-Meier estimates). C, Effect of N factor of primary CRC on RFS after curative pulmonary resection (Kaplan-Meier estimates). D, Effect of preoperative CEA level on RFS after curative pulmonary resection (Kaplan-Meier estimates).

Supplementary Figure S3.

A, Kaplan-Meier curves of OS in CRC patients after pulmonary resection (Kaplan-Meier estimates). B, Effects of CCL15 expression on OS in CRC patients after pulmonary resection with lung metastases (Kaplan-Meier estimates).

Supplementary Figure S4.

Simultaneous immunofluorescence staining for CCR1 (red) and CD3 (A), CD8 (B), CD68 (C), α-SMA (D), CD14 (E), or CXCR2 (F) (green). Scale bar, 20 μm.

Supplementary Figure S5.

Simultaneous immunofluorescence staining for CCR1 (red) and CD11b (A), CD33 (B),

HLA-DR (C), or CD15 (D) (green). Scale bar, 20 μm.

Supplementary Figure S6.

Characterization of $CCR1^+$ cells in the tumor microenvironment of CRC liver metastases. Simultaneous immunofluorescence staining for CCR1 (red) and MPO (A), CD11b (B), CD33 (C), HLA-DR (D), CD15 (E), CD16 (F), ARG1 (G) or MMP9 (H) (green). Scale bar, 20 μm.

Supplementary Figure S1

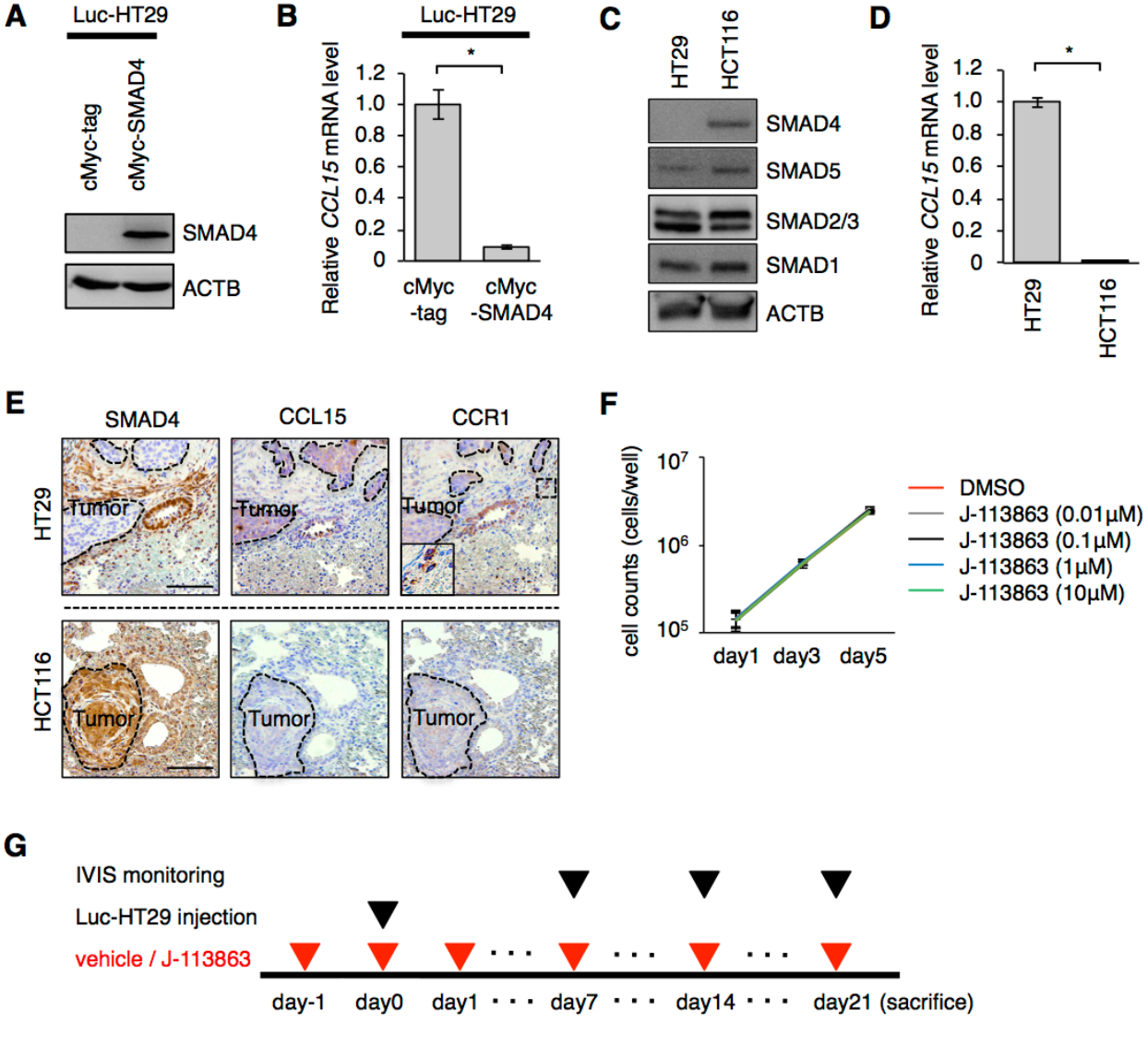

H

vehicle	day7	day14	day21
#1	1	2.56	17.59
#2	1	0.30	50.52
#3	1	0.63	0.10
#4	1	1.15	10.66
#5	1	0.49	22.31
#6	1	1.89	1.45
mean ± SD	1	1.17 ± 0.89	17.11 ± 18.54

J-113863	day7	day14	day21
#1	1	1.38	0.96
#2	1	2.02	0.46
#3	1	1.99	17.35
#4	1	1.00	12.43
#5	1	1.56	1.39
#6	1	0.37	0.56
#7	1	0.31	1.17
#8	1	0.56	10.05
mean ± SD	1	1.15 ± 0.69	5.54 ± 6.71

Supplementary Figure S2

A

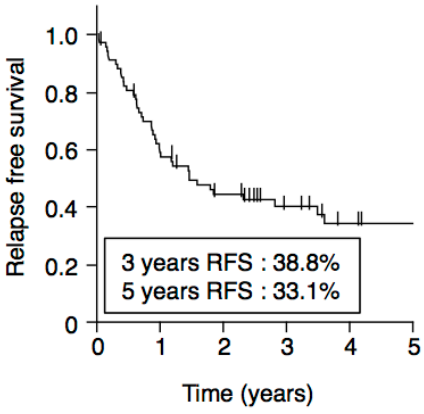

No. of patients						
	67	40	26	16	10	8

B

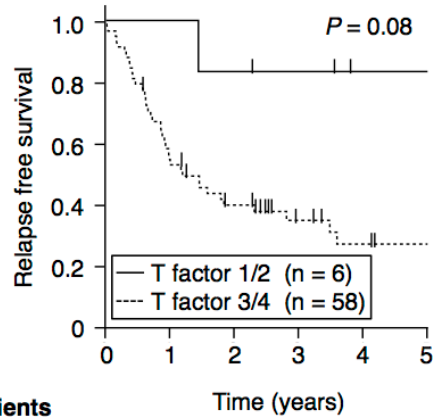

No. of patients						
T factor 1/2	6	6	5	4	2	2
T factor 3/4	58	33	20	11	7	5

C

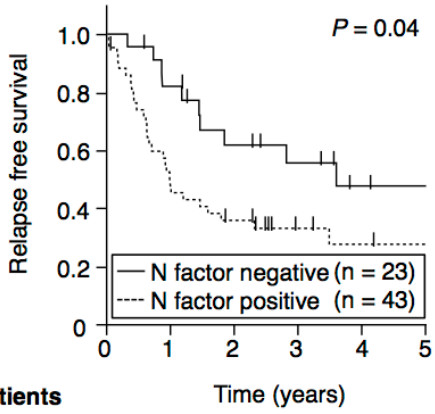

No. of patients						
N factor negative	23	18	12	9	5	4
N factor positive	43	22	14	7	5	4

D

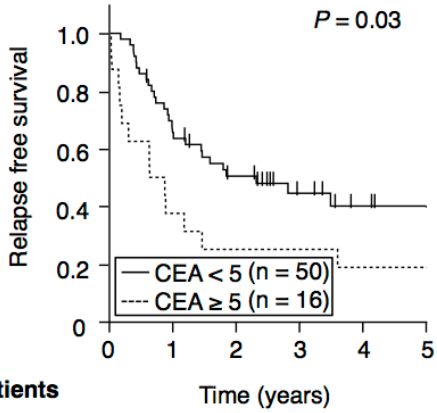

No. of patients						
CEA < 5	50	34	22	12	7	5
CEA ≥ 5	16	6	4	4	3	3

Supplementary Figure S3

A

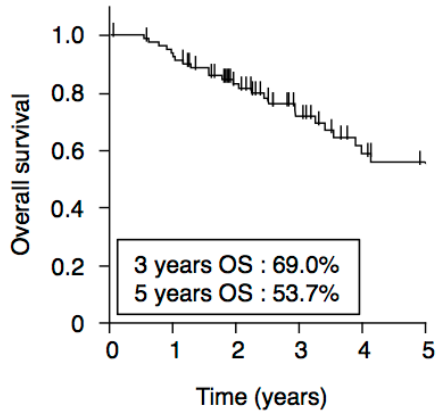

No. of patients	81	74	53	33	22	17

B

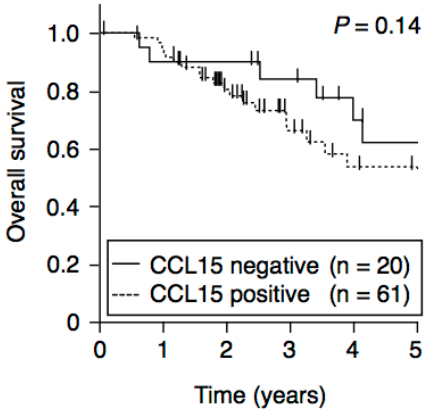

No. of patients						
CCL15 negative	20	18	17	14	10	7
CCL15 positive	61	56	36	19	12	10

Supplementary Figure S4

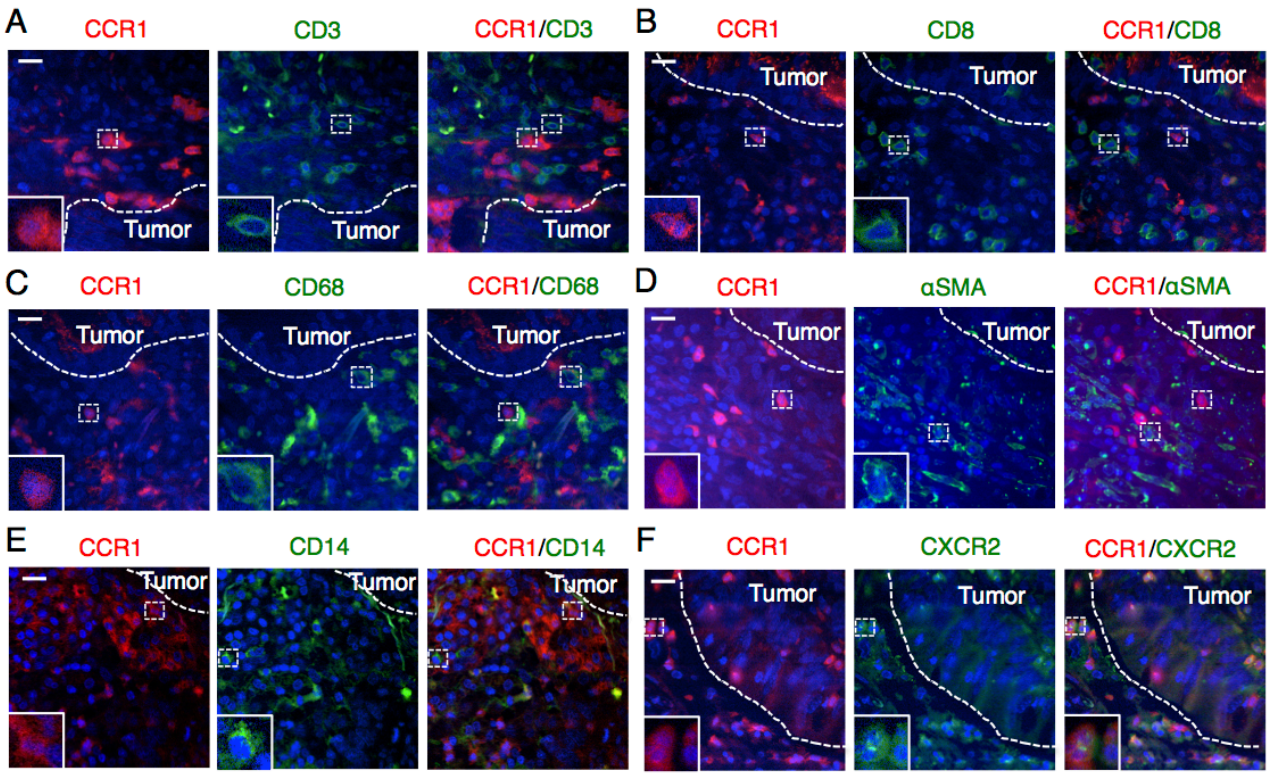

Supplementary Figure S5

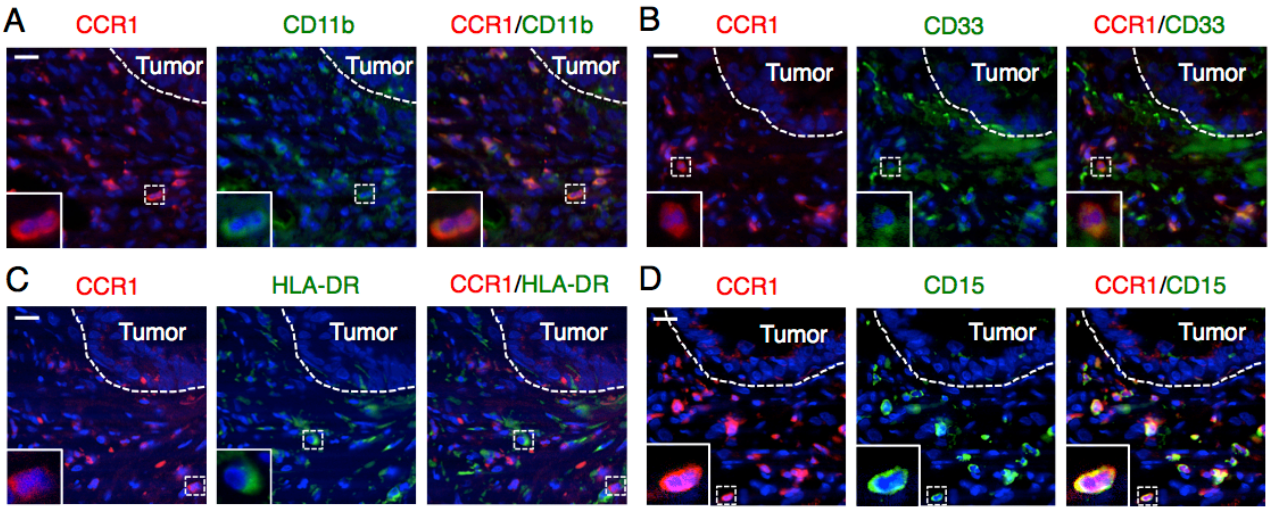

Supplementary Figure S6